

The kinase domain of CK1 enzymes contains the localization cue essential for compartmentalized signaling at the spindle pole

Zachary C. Elmore, Rodrigo X. Guillen, and Kathleen L. Gould*

Department of Cell and Developmental Biology, Vanderbilt University School of Medicine, Nashville, TN 37232

ABSTRACT CK1 protein kinases contribute to multiple biological processes, but how they are tailored to function in compartmentalized signaling events is largely unknown. Hhp1 and Hhp2 (Hhp1/2) are the soluble CK1 family members in *Schizosaccharomyces pombe*. One of their functions is to inhibit the septation initiation network (SIN) during a mitotic checkpoint arrest. The SIN is assembled by Sid4 at spindle pole bodies (SPBs), and though Hhp1/2 colocalize there, it is not known how they are targeted there or whether their SPB localization is required for SIN inhibition. Here, we establish that Hhp1/2 localize throughout the cell cycle to SPBs, as well as to the nucleus, cell tips, and division site. We find that their catalytic domains but not their enzymatic function are used for SPB targeting and that this targeting strategy is conserved in human CK1 δ/ϵ localization to centrosomes. Further, we pinpoint amino acids in the Hhp1 catalytic domain required for SPB interaction; mutation of these residues disrupts Hhp1 association with the core SPB protein Ppc89, and the inhibition of cytokinesis in the setting of spindle stress. Taken together, these data have enabled us to define a molecular mechanism used by CK1 enzymes to target a specific cellular locale for compartmentalized signaling.

Monitoring Editor

Daniel J. Lew
Duke University

Received: Feb 20, 2018

Revised: May 2, 2018

Accepted: May 3, 2018

INTRODUCTION

Casein kinases are among the most abundant serine/threonine protein kinases found in eukaryotic cells (Desjardins *et al.*, 1972; Matsuura and Takeda, 1972; Hathaway and Traugh, 1979; Tuazon and Traugh, 1991; Carpy *et al.*, 2014) and generally recognize substrate motifs consisting of acidic or phosphorylated amino acid residues (Agostinis *et al.*, 1989; Flotow *et al.*, 1990; Flotow and Roach, 1991; Meggio *et al.*, 1991, 1992; Graves *et al.*, 1993). Members of the casein kinase 1 (CK1) family have been implicated in multiple cellular processes, including regulation of autophagy, DNA repair, circadian rhythm, ribosome assembly, intracellular trafficking, meiotic

progression, and Wnt signaling (Knippschild *et al.*, 2005; Schitteck and Sinnberg, 2014; Ghalei *et al.*, 2015; Nakatogawa, 2015). CK1 kinases share highly related catalytic domains (53–98% sequence identity) that consist of a bilobed structure with a smaller N-terminal lobe consisting primarily of β -sheets and a larger, primarily α -helical C-terminal lobe (Carmel *et al.*, 1994; Xu *et al.*, 1995; Longenecker *et al.*, 1996). However, CK1 family members have divergent C-terminal noncatalytic domains that are thought to dictate intracellular localization and govern catalytic activity (Graves and Roach, 1995; Longenecker *et al.*, 1996, 1998; Cegielska *et al.*, 1998; Gietzen and Virshup, 1999; Babu *et al.*, 2002; Dahlberg *et al.*, 2009; Greer and Rubin, 2011; lanes *et al.*, 2015; Meng *et al.*, 2016). Indeed, some CK1 isoforms are anchored to membranes via C-terminal palmitoylation (Wang *et al.*, 1992; Vancura *et al.*, 1994; Babu *et al.*, 2004; Sun *et al.*, 2004).

Hhp1 and Hhp2 (hereafter referred to as Hhp1/2) are the sole soluble CK1s in *Schizosaccharomyces pombe* and are orthologues of *Saccharomyces cerevisiae* Hrr25p and human CK1 δ and CK1 ϵ (hereafter referred to as CK1 δ/ϵ) (Dhillon and Hoekstra, 1994; Hoekstra *et al.*, 1994). In addition to functioning redundantly in meiosis, DNA damage repair, and mitotic commitment (Dhillon and Hoekstra, 1994; Sakuno and Watanabe, 2015; Chan *et al.*, 2017), Hhp1/2 are essential for preventing cytokinesis during a

This article was published online ahead of print in MBoC in Press (<http://www.molbiolcell.org/cgi/doi/10.1091/mbc.E18-02-0129>) on May 9, 2018.

*Address correspondence to: Kathleen L. Gould (kathy.gould@vanderbilt.edu).

Abbreviations used: ANOVA, analysis of variance; CK1, casein kinase 1; CK1 δ/ϵ , human CK1 δ and CK1 ϵ ; GFP, green fluorescent protein; Hhp1/2, Hhp1 and Hhp2; HU, hydroxyurea; IgG, immunoglobulin G; KDE, kinase domain extension; mNG, mNeonGreen; ORF, open reading frame; ROI, region of interest; SIN, septation initiation network; SPB, spindle pole body; YE, yeast extract.

© 2018 Elmore *et al.* This article is distributed by The American Society for Cell Biology under license from the author(s). Two months after publication it is available to the public under an Attribution–Noncommercial–Share Alike 3.0 Unported Creative Commons License (<http://creativecommons.org/licenses/by-nc-sa/3.0>).

“ASCB®,” “The American Society for Cell Biology®,” and “Molecular Biology of the Cell®” are registered trademarks of The American Society for Cell Biology.

mitotic stress imposed by microtubule depolymerization (Johnson *et al.*, 2013). In this checkpoint pathway, Hhp1/2 function redundantly upstream of the ubiquitin ligase Dma1 to inhibit the septation initiation network (SIN) (Murone and Simanis, 1996; Guertin *et al.*, 2002b), a *hippo*-related signaling pathway localized at the spindle pole body (SPB) that triggers cytokinesis (Johnson and Gould, 2011; Johnson *et al.*, 2012; Simanis, 2015). Specifically, Hhp1/2 phosphorylate the SIN scaffold Sid4 at T275 and S278 to create a docking site for Dma1's FHA domain (Johnson *et al.*, 2013). Dma1 then concentrates at SPBs and ubiquitinates Sid4, also a scaffold for Polo-like kinase Plo1, to inhibit Plo1's SPB localization and ability to activate the SIN (Guertin *et al.*, 2002; Johnson and Gould, 2011).

In addition to other subcellular localizations, Hhp1/2, as well as Hrr25p and human CK1δ/ε, localize to the SPB or its equivalent in vertebrates, the centrosome (Hutchins *et al.*, 2010; Greer and Rubin, 2011; Johnson *et al.*, 2013; Peng *et al.*, 2015b). Interaction with AKAP450 and the γ-tubulin complex is reported to be important for anchoring CK1δ and Hrr25p to the centrosome and SPB, respectively (Sillibourne *et al.*, 2002; Peng *et al.*, 2015b). However, the residues within CK1 enzymes required for SPB/centrosome recruitment are unknown, as is the SPB tether in *S. pombe*.

In this work, we establish that Hhp1/2 localize throughout the cell cycle to the SPB and also to the nucleus and cell division site, with Hhp2 showing additional localization to cell tips. We report that the catalytic domains of Hhp1/2 are sufficient to support this localization pattern independently of enzymatic function. Further, we define conserved residues at the base of the Hhp1 catalytic domain necessary for SPB localization. Mutation of these residues eliminates Hhp1's SPB localization and mitotic checkpoint function by disrupting the interaction with the core SPB protein Ppc89 (Rosenberg *et al.*, 2006) but does not affect other critical Hhp1 functions. We also find that the centrosomal targeting information in human CK1δ/ε is analogously contained within their respective kinase domains, indicating conservation of this localization mechanism from yeast to humans. This study provides novel insight into how specific docking residues within the catalytic domain of protein kinases can direct them to subcellular locations to control substrate phosphorylation and downstream signaling.

RESULTS

Hhp1/2 localization during a normal and perturbed cell cycle

Both Hhp1 and Hhp2 localize to SPBs, and either is sufficient to promote the Dma1-mediated mitotic checkpoint that delays cytokinesis (Johnson *et al.*, 2013). For determination of their intracellular distribution throughout the cell cycle and during a mitotic arrest, each was tagged at its endogenous C-terminus with mNeonGreen (mNG) (Shaner *et al.*, 2013; Willet *et al.*, 2015) and coimaged with the SPB protein Sid4-RFP (Chang and Gould, 2000). Both Hhp1 and Hhp2 localize to the nucleus and the division site in addition to SPBs; Hhp2 was also detected at cell tips (Figure 1A). By immunoblotting whole-cell lysates from a strain producing both enzymes tagged with green fluorescent protein (GFP), we determined that Hhp1 is more abundant than Hhp2 (Supplemental Figure S1A), consistent with the relative protein levels determined by quantitative mass spectrometry (Marguerat *et al.*, 2012; Carpy *et al.*, 2014) and the more severe growth defects and phenotypes associated with the deletion of *hhp1*⁺ relative to *hhp2*⁺ (Supplemental Figure S1, B–D) (Dhillon and Hoekstra, 1994; Hoekstra *et al.*, 1994; Bimbo *et al.*, 2005; Carpy *et al.*, 2014; Chen *et al.*, 2015). To better define the localization of Hhp1/2 during the mitotic checkpoint signaling

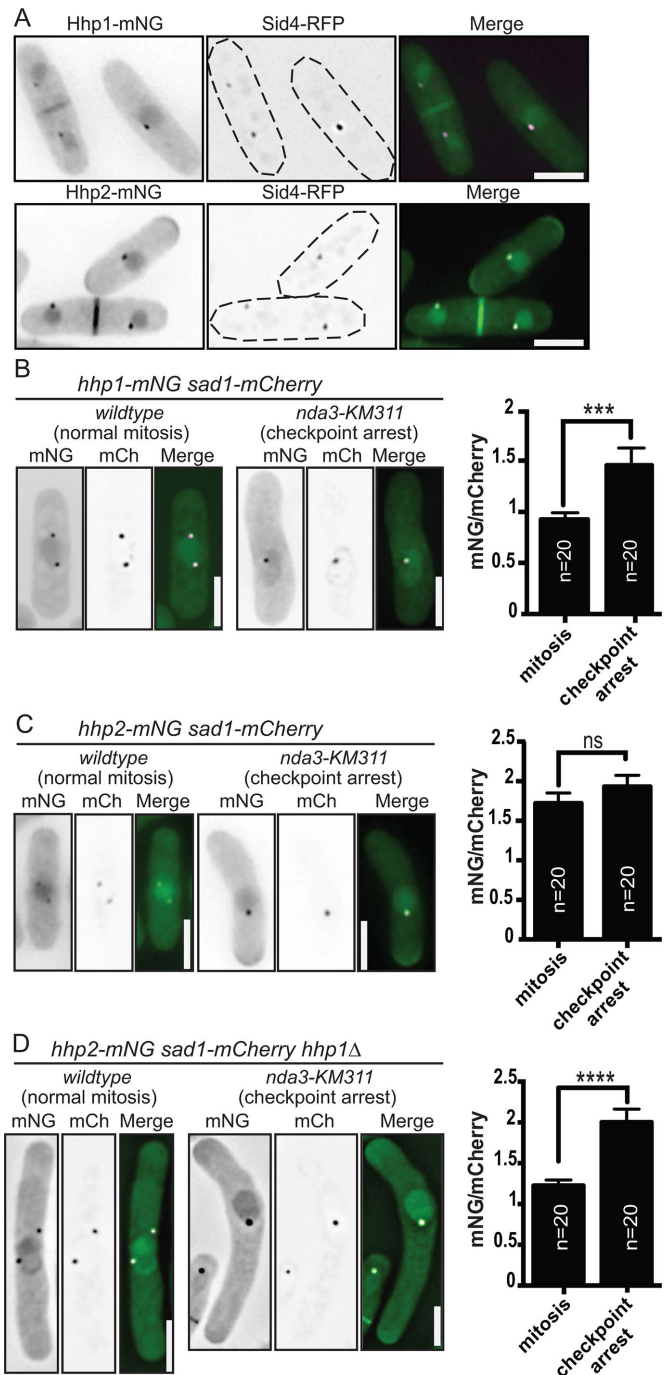


FIGURE 1: Intracellular localization patterns of Hhp1/2. (A) Live-cell imaging of Hhp1-mNG and Hhp2-mNG with Sid4-RFP. (B–D) Hhp1-mNG (B) and Hhp2-mNG (C, D) were imaged in prometaphase-arrested and wild-type mitotic *sad1-mCherry* or *sad1-mCherry hhp1Δ* cells. Representative inverted grayscale images are shown in the left panels with quantitation to the right. mCh, mCherry. Scale bars: 5 μm. Values are represented as mNG/mCherry intensity ratios. ***, $p < 0.005$, ****, $p < 0.001$ determined using Student's *t* test. ns, not significant. Error bars represent SEM.

window, we performed time-lapse imaging of cells progressing through mitosis. Hhp1-mNG and Hhp2-mNG localized to the SPB and nucleus throughout mitosis, and also to the division site following the completion of spindle elongation with comparable timing (Supplemental Figure S1, E and F). These data indicate that the

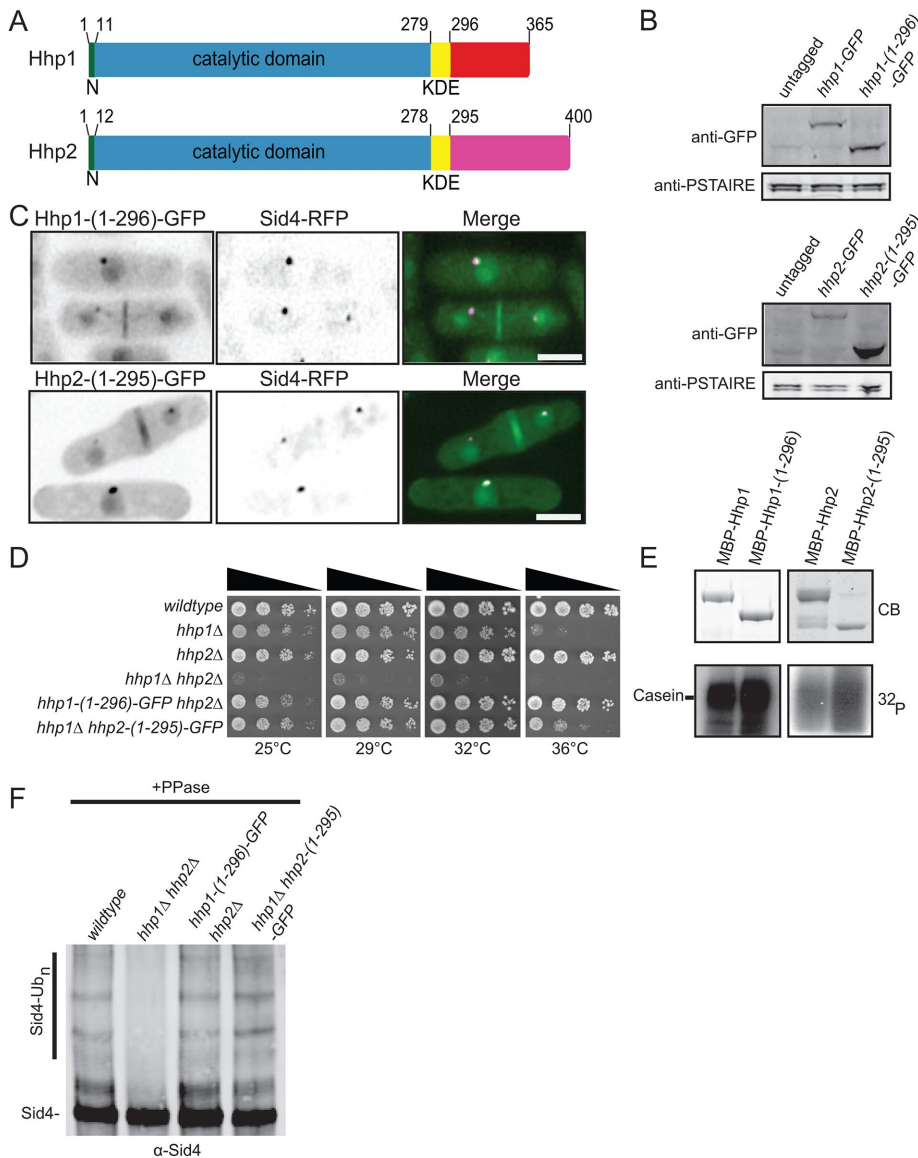


FIGURE 2: The C-termini of Hhp1/2 are dispensable for their functions. (A) Schematic diagrams of Hhp1/2 with relative positions of N-terminal extensions (N, green), kinase domains (blue), kinase domain extensions (KDE, yellow), and unrelated C-termini in red or purple indicated, drawn to scale. (B) Anti-GFP immunoblots of whole-cell extracts prepared from untagged and the indicated GFP-tagged strains. Anti-PSTAIRE (Cdc2) immunoblots served as protein loading controls. (C) Live-cell imaging of endogenously tagged Hhp1-(1-296)-GFP and Hhp2-(1-295)-GFP with Sid4-RFP. Scale bars: 5 μ m. (D) Serial 10-fold dilutions of the indicated strains were spotted on YE plates and incubated at the indicated temperatures. (E) In vitro kinase assays of recombinant MBP-Hhp1, MBP-Hhp1-(1-296), MBP-Hhp2, and MBP-Hhp2-(1-295) detected by Coomassie blue (CB) staining of SDS-PAGE gels, with casein as substrate. Phosphorylated casein was detected by autoradiography (32 P). (F) Sid4 from the indicated strains was immunoprecipitated from denatured cell lysates, treated with phosphatase, and visualized by immunoblotting.

spatial and temporal distributions of Hhp1 and Hhp2 are similar but not identical.

When the mitotic checkpoint is activated by preventing microtubule polymerization in the *nda3-KM311 β* -tubulin mutant (Toda et al., 1983), Sid4 is phosphorylated by Hhp1/2, and Hhp1 increases in intensity at SPBs (Johnson et al., 2013) (Figure 1B). By coimaging with the SPB marker Sad1-mCherry in checkpoint-activated and unperturbed mitotic cells, we found that Hhp2 intensity at duplicated but unseparated SPBs was also increased in checkpoint-activated

cells, but only if they lacked Hhp1 (Figure 1, C and D). These results indicate that both Hhp1/2 can accumulate at SPBs during the checkpoint.

Hhp1/2 catalytic domains direct SPB localization and checkpoint function

To determine the mechanism of Hhp1/2 SPB targeting, we first defined the regions of the enzymes necessary for this localization. Hhp1/2 contain conserved N-terminal catalytic domains and kinase domain extensions (KDEs) that are conserved among mammalian but not *S. cerevisiae* CK1 family members (reviewed in Knippschild et al., 2014) (Figure 2A). Given that both Hhp1/2 localize to SPBs and participate in checkpoint signaling, we anticipated that homologous sequences dictated these functions and that their unrelated C-termini were not involved. Accordingly, Hhp1/2 C-terminal truncations, constructed by inserting sequences encoding GFP in the endogenous *hhp1/2* loci to produce Hhp1-(1-296)-GFP and Hhp2-(1-295)-GFP (Figure 2B), both co-localized with Sid4-RFP at SPBs (Figure 2C). Moreover, Hhp1-(1-296)-GFP and Hhp2-(1-295)-GFP recapitulated all other subcellular localizations of the full-length proteins (Figure 2C). The C-terminus of Hhp1 fused to GFP was not targeted to any particular subcellular location, although it was produced in cells (Supplemental Figure S2, A and B), indicating that the C-terminus is neither necessary nor sufficient for SPB localization of Hhp1/2.

To ascertain the functionality of the C-terminal truncation mutants of Hhp1/2, we performed growth, in vitro kinase, and mitotic checkpoint assays. First, we found that each of the *hhp1/2* C-terminal truncation mutants integrated as the sole *hhp1/2* allele in cells rescued the severe growth defect of the double-deletion mutant in vivo (Figure 2D). Consistent with this finding and previous reports (Graves and Roach, 1995; Cegielska et al., 1998; Gietzen and Virshup, 1999), recombinant Hhp1/2 C-terminal truncation mutants phosphorylated the exogenous substrate casein in vitro even more robustly than the full-length proteins (Figure 2E). Importantly, we found that the truncation mutants were sufficient to inhibit the SIN during the mitotic checkpoint. GFP-tagged Hhp1 and Hhp2 C-terminal truncations accumulated at SPBs during a mitotic checkpoint arrest (Supplemental Figure S2, C and D), and Sid4 was appropriately ubiquitinated (Figure 2F). Taken together, these data indicate that the C-termini of Hhp1/2 are dispensable for their SPB localization and function during the Dma1-mediated mitotic checkpoint.

Because the KDE of CK1 δ was reported to mediate its centrosomal localization (Greer and Rubin, 2011), we tested whether

Hhp1/2 KDEs influence SPB targeting. Further C-terminal truncations of Hhp1/2 were made such that only the predicted catalytic domains (Hhp1-(1-280)-GFP and Hhp2-(1-278)-GFP) were produced from endogenous loci (Supplemental Figure S3A). While these Hhp1/2 truncation mutants were still SPB targeted, as evidenced by colocalization with Sid4-RFP (Supplemental Figure S3B), functional tests revealed that they only partially rescued the severe growth defect of the double-deletion mutant in vivo (Supplemental Figure S3C), and they did not support mitotic checkpoint signaling as assayed by Sid4 ubiquitination (Supplemental Figure S3D). This loss of in vivo function is likely due to significantly reduced kinase activity (Supplemental Figure S3, E and F). We conclude that, while the KDEs of Hhp1/2 are required for their full enzymatic function, SPB targeting information is contained within the Hhp1/2 catalytic domains.

Hhp1/2 localize to SPBs independent of catalytic activity

It was previously reported that the kinase activity of CK1 δ and of Hrr25 is necessary for their proper centrosomal and SPB localization, respectively (Milne *et al.*, 2001; Peng *et al.*, 2015a,b). Because the Hhp1-(1-280)-GFP and Hhp2-(1-278)-GFP mutants had severely reduced activity but were still able to localize, we hypothesized that, in contrast, Hhp1/2 kinase activity may not impact their SPB targeting. We generated catalytically inactive mutants of each enzyme (Hhp1-K40R and Hhp2-K41R) and verified their inactivity in vitro (Figure 3A). When produced at the endogenous loci as sole gene copies tagged with mNG in cells, these mutants mimicked null alleles in growth and Sid4 ubiquitination assays (Supplemental Figure S4, A and B), although they were produced at wild-type levels as determined by immunoblotting (Figure 3B) and by measuring whole-cell fluorescence intensities (Supplemental Figure S4, C and D). Coimaging of Sid4-RFP and Hhp1-(K40R)-mNG or Hhp2-(K41R)-mNG showed that both catalytically inactive mutants localized to SPBs (Figure 3C), indicating that Hhp1/2 kinase activity is not necessary for SPB localization. Furthermore, Hhp1-(K40R)-mNG colocalized with Sid4-RFP in a *hhp2* Δ background, and Hhp2-(K41R)-mNG colocalized with Sid4-RFP in a *hhp1* Δ background. Taken together, these data indicate that *hhp2* is not required for the SPB localization of Hhp1 and vice versa.

The kinase domains of CK1 δ/ϵ dictate centrosomal localization

CK1 δ/ϵ , the vertebrate orthologues of Hhp1/2, localize to the centrosome (Milne *et al.*, 2001; Hutchins *et al.*, 2010) (Figure 4A). To determine whether the intrinsic cues necessary for Hhp1/2 SPB localization are conserved in CK1 δ/ϵ , we made C-terminal truncations of CK1 δ/ϵ analogous to those of Hhp1/2 that did or did not contain the KDE (Supplemental Figure S5A). These truncation mutants or wild-type versions of the proteins were then expressed in RPE-1 cells as N-terminal GFP fusions (Figure 4A and Supplemental Figure S5B). In the majority of transfected cells, all three versions of the proteins colocalized with the centrosomal marker γ -tubulin, although truncation of the KDE from either protein resulted in a lower percentage of centrosomal localization compared with wild type or truncations including the KDEs (Figure 4, A and B). These data support the idea that, as in Hhp1/2, the centrosome-targeting information is contained within the CK1 δ/ϵ kinase domains, and we hypothesize that the KDE may impart stability to their association with centrosomes.

We next tested whether kinase activity was important for CK1 δ/ϵ centrosomal localization. K38R mutations in both enzymes render them inactive (Gietzen and Virshup, 1999) (Supplemental Figure S5C). When these mutations were expressed in RPE-1 cells as GFP

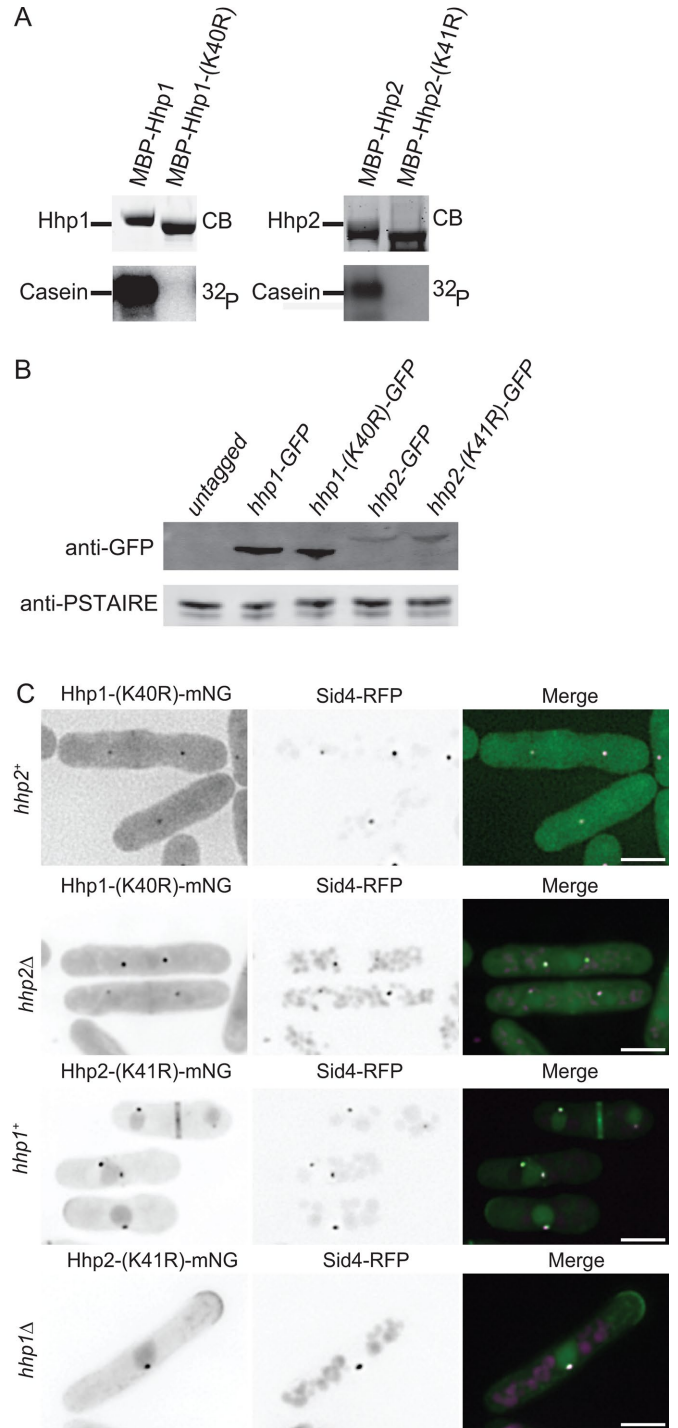


FIGURE 3: Kinase activity of Hhp1/2 is not required for SPB localization. (A) In vitro kinase assays of recombinant MBP-Hhp1-(K40R) and MBP-Hhp2-(K41R) detected by CB staining of SDS-PAGE gels, with casein as substrate. Phosphorylated casein was detected by autoradiography. (B) Anti-GFP immunoblot of whole-cell extracts prepared from untagged and the indicated GFP-tagged strains. Anti-PSTAIRES antibody served as loading control for lysates. (C) Live-cell imaging of endogenously tagged Hhp1-(K40R)-mNG with Sid4-RFP in *wildtype* and *hhp2* Δ cells along with Hhp2-(K41R)-mNG with Sid4-RFP in *wildtype* and *hhp1* Δ cells. Scale bars: 5 μ m.

fusions (Supplemental Figure S5D), both colocalized at centrosomes with γ -tubulin to the same extent as wild type (Figure 4, C–E), indicating that protein kinase activity is dispensable for their

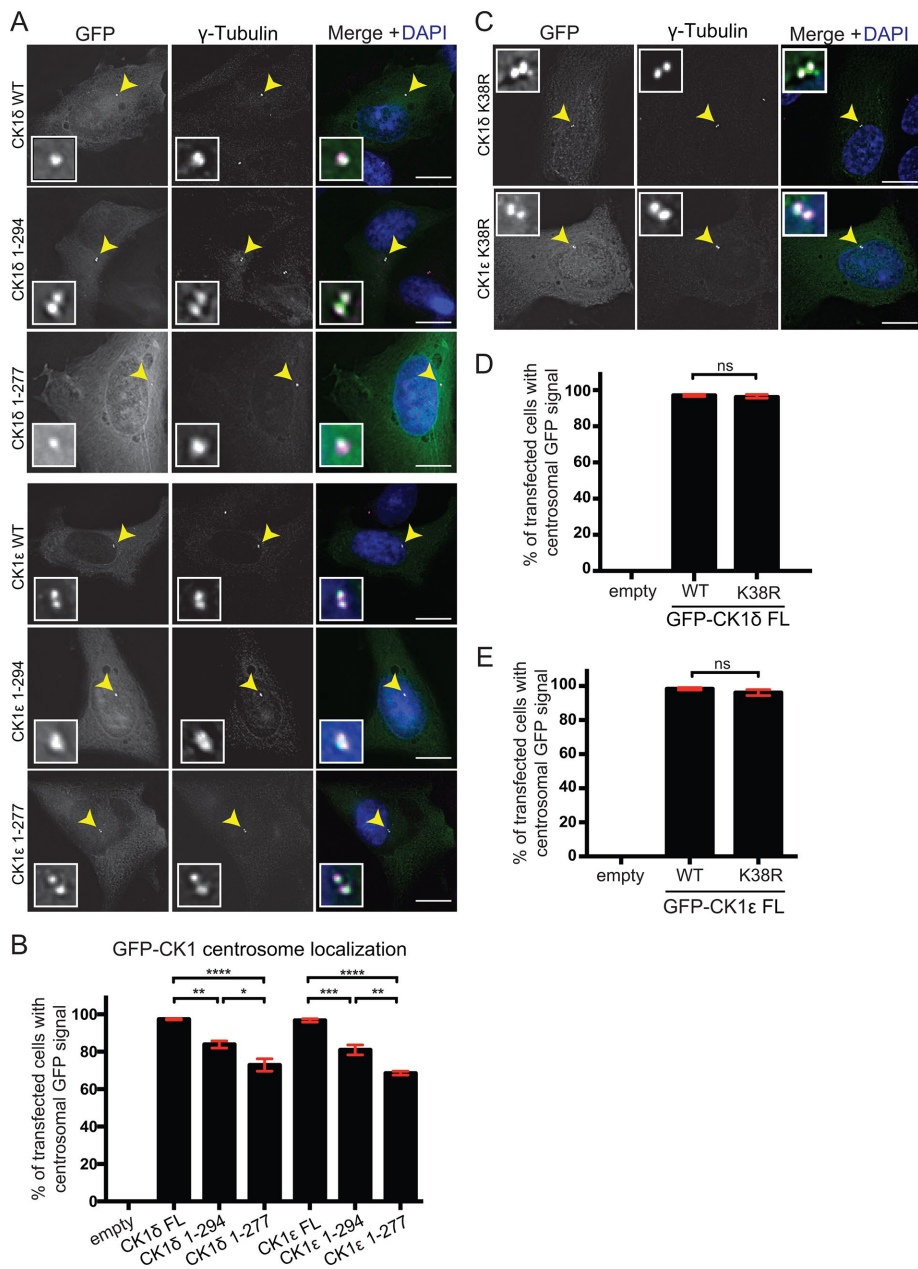


FIGURE 4: The centrosomal targeting information of CK1 δ/ϵ is located within the kinase domain. RPE-1 cells were transiently transfected with GFP N-terminal fusions to full length or truncations of CK1 δ and CK1 ϵ . Cells were fixed with 100% methanol and stained with γ -tubulin (magenta) and DAPI (blue). (A) Localization of full-length protein and truncation mutants in RPE-1 cells. (B) Quantification of the colocalization between γ -tubulin and full-length proteins or truncation mutants. (C) Localization of full-length GFP-CK1 δ and GFP-CK1 ϵ catalytically inactive mutants. (D, E) Quantification of the colocalization between γ -tubulin and GFP-CK1 δ (D) or GFP-CK1 ϵ (E) wild type or catalytically inactive mutants. For B, D, and E, 100 cells per experiment. $n = 3$. *, $p < 0.05$, **, $p < 0.01$, ***, $p < 0.005$, ****, $p < 0.001$, p values determined using ANOVA; ns, not significant. Error bars represent SEM. Scale bars: 15 μm .

centrosomal targeting. Taken together, these data indicate that soluble CK1 family members use their catalytic domains to associate with the major microtubule organizing centers.

Residues in the C-terminal lobe of the Hhp1 kinase domain are required for SPB localization

To probe the mechanism by which one of these enzymes targets spindle poles, we identified residues in the Hhp1 catalytic domain

that were necessary. To do this, we performed a comparative analysis of Hhp1 and its paralogue, Cki2. Cki2 does not localize to SPBs; Cki2 C-terminally tagged with GFP localized to vacuolar membranes (Supplemental Figure S6, A and B, top), as previously reported (Matsuyama *et al.*, 2006). Furthermore, a C-terminally tagged mutant of Cki2 lacking the predicted palmitoylation sites (Cki2-(1-429)-GFP) (Sun *et al.*, 2004) localized to the nucleus, cytoplasm, and division site, but it still did not localize to SPBs (Supplemental Figure S6, A and B, bottom), indicating that Cki2 lacks SPB-targeting information.

To detect differences between Hhp1 and Cki2, we generated structural models of the kinase domains of Hhp1 and Cki2 (Figure 5A and Supplemental Figure S6C) using the Protein Homology/analogy Recognition Engine v. 2.0 (Phyre²) (Kelley *et al.*, 2015). A comparison revealed 19 surface residues of Cki2 that differed in charge potential from analogous residues on Hhp1 (Supplemental Figure S6, C and D). To determine whether any of these residues mediate SPB localization, the corresponding residues in Hhp1 were mutated to either mimic the Cki2 residue or reverse the charge of the Hhp1 residue, and the resultant mutants were integrated at the *hhp1* endogenous locus and tagged at their C-termini with mNG. Of the 14 mutants tested, only Hhp1-(R261E)-mNG and Hhp1-(R272E K273E)-mNG failed to localize to SPBs (Figure 5B and Supplemental Figure S6D). Hhp1-(R261E)-mNG and Hhp1-(R272E K273E)-mNG were still recruited to other subcellular locations, including the nucleus and division site. Both mutant proteins were produced at levels similar to those of wild type (Figure 5C). Interestingly, these mutants retained function, as measured by their ability to support wild-type *S. pombe* growth and phosphorylate casein *in vitro* (Supplemental Figure S6, E and F).

Interaction with Ppc89 mediates Hhp1/2 SPB localization

Though Sid4 is an SPB-localized Hhp1/2 target (Johnson *et al.*, 2013), Sid4 is not required for Hhp1 (Johnson *et al.*, 2013) or Hhp2 (Supplemental Figure S7A) SPB localization, and it is not known which protein(s)

tethers Hhp1/2 to SPBs. However, Hhp1/2 copurify with multiple SPB proteins, including a central component of the SPB, Ppc89, which also secures Sid4 at the SPB (Rosenberg *et al.*, 2006; Johnson *et al.*, 2013). Ppc89 is required for Hhp1 (Johnson *et al.*, 2013) and Hhp2 (Supplemental Figure S7B) SPB localization, and *ppc89* interacts with *hhp1* (Vo *et al.*, 2016) and *hhp2* in a yeast two-hybrid assay (Figure 6, A–C). We further determined that a C-terminal truncation of Ppc89 supports two-hybrid interactions with *hhp1/2* (Figure 6A),

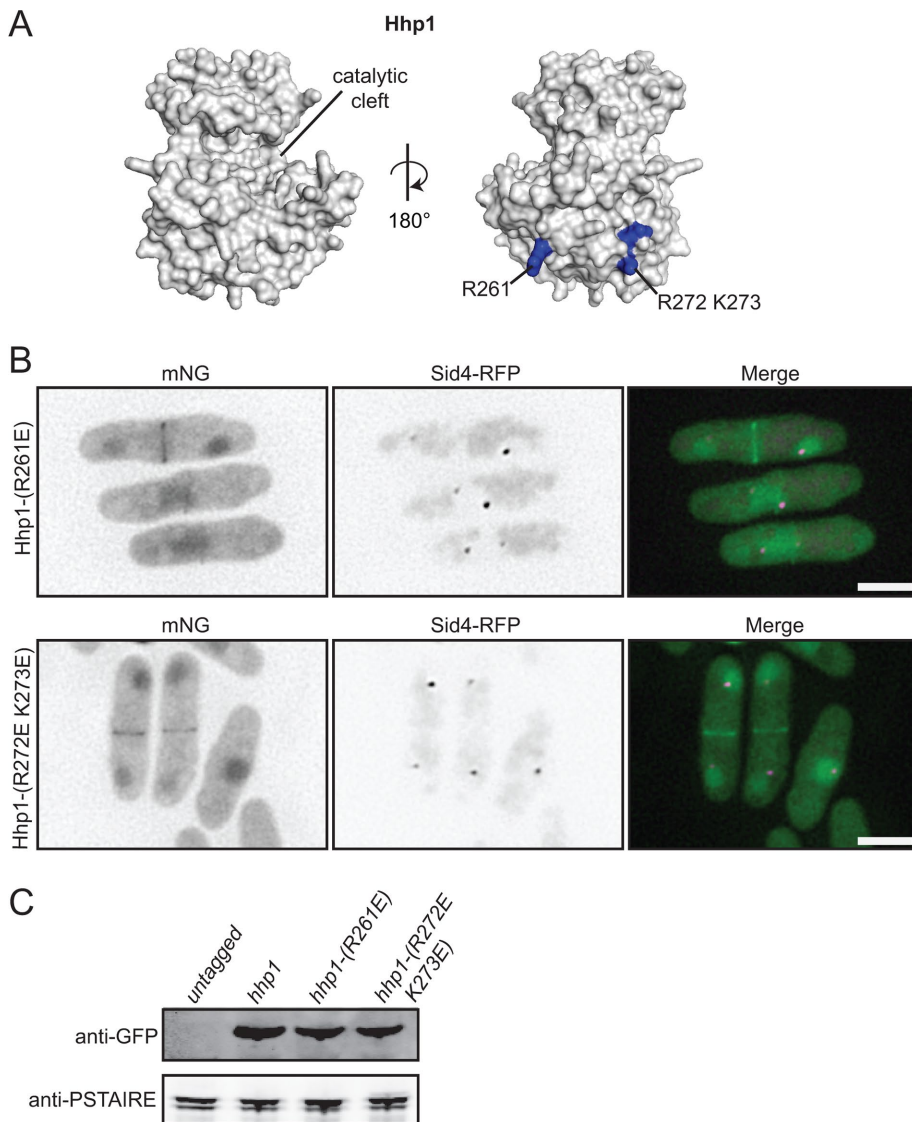


FIGURE 5: Residues at the base of the Hhp1 catalytic domain are critical for SPB localization. (A) Homology model of Hhp1 catalytic domain generated from Phyre² software and visualized with MacPymol. Residues critical for Hhp1 SPB localization are in blue. (B) Live-cell imaging of endogenously tagged Hhp1-(R261E)-mNG and Hhp1-(R272E K273E)-mNG with Sid4-RFP. Scale bars: 5 μ m. (C) Anti-GFP immunoblot of whole-cell extracts prepared from the indicated strains. Anti-PSTAIRE immunoblots served as protein loading controls.

indicating that the interaction site is distinct from that of Sid4, which interacts with the Ppc89 C-terminus (Rosenberg *et al.*, 2006).

We next tested whether the residues that were critical for Hhp1 SPB localization affected interaction with Ppc89. We found that neither *hhp1-R261E* nor *hhp1-R272E K273E* interacted with *ppc89* in the two-hybrid assay (Figure 6, B and C). Thus, these residues likely mediate an interaction with Ppc89, which may position Hhp1/2 proximal to their mitotic checkpoint substrate, Sid4.

Hhp1/2 SPB localization is required for checkpoint signaling

To test the hypothesis that CK1 must be present at SPBs to execute its checkpoint function, we examined the ability of Hhp1-R261E and Hhp1-R272E K273E to prevent septation when a mitotic checkpoint is imposed. Because either Hhp1 or Hhp2 can redundantly activate the Dma1-mediated mitotic checkpoint, we combined *hhp1-R261E* and *hhp1-R272E K273E* with an *hhp2 Δ* mutant to

analyze mitotic checkpoint function. We found that the tubulin mutant *nda3-KM311*, *nda3-KM311 hhp1-(R272E K273E)* and *nda3-KM311 hhp1-(R261E)* delayed septation, whereas *nda3-KM311 hhp1-(R272E K273E) hhp2 Δ* and *nda3-KM311 hhp1-(R261E) hhp2 Δ* could not hold the arrest (Figure 7, A and B). Because of its ability to inhibit the SIN via Sid4 ubiquitination, overexpression of *dma1* is lethal (Guertin *et al.*, 2002); however, *hhp1-(R261E) hhp2 Δ* and *hhp1-(R272E K273E) hhp2 Δ* mutants were refractory to *dma1* overexpression-induced lethality (Figure 7C). Also consistent with checkpoint failure, Sid4 ubiquitination was not detected in checkpoint-activated *hhp1-(R261E) hhp2 Δ* or *hhp1-(R272E K273E) hhp2 Δ* cells (Figure 7D). Taken together, these data indicate that Hhp1/2 localization to SPBs is critical for their role in mitotic checkpoint signaling.

DISCUSSION

The mechanisms governing CK1 enzyme targeting to specific intracellular locales are not well defined. The *S. pombe* CK1 enzymes Hhp1/2 are the most upstream components yet identified in the Dma1-mediated mitotic checkpoint that stalls cytokinesis when the mitotic spindle is disrupted. To define how they access their SPB substrate Sid4 in this pathway, we determined how they localize to SPBs and whether this was an essential feature of the checkpoint pathway. We found that Hhp1/2 catalytic domains but not enzymatic activities provide the localization cue and that this targeting strategy is conserved in human CK1 δ/ϵ localization to centrosomes. In further probing the specific requirements for spindle pole localization in one of these enzymes, we identified positively charged residues at the base of the Hhp1 catalytic domain that support interaction with a key SPB scaffold, Ppc89. This interaction is necessary for Hhp1 SPB association, Sid4 phosphorylation, and a mitotic checkpoint response, but not for other functions carried out by this enzyme to promote cell proliferation. Our findings reveal a conserved mechanism by which CK1 enzymes can be tailored to perform a specific function at a discrete subcellular location and time.

Our findings reveal a conserved mechanism by which CK1 enzymes can be tailored to perform a specific function at a discrete subcellular location and time.

Hhp1/2 have overlapping but not identical subcellular localizations

Hhp1/2 have redundant roles in the Dma1-dependent mitotic checkpoint (Johnson *et al.*, 2013), and deletion of either enzyme also renders cells sensitive to multiple types of DNA-damaging agents (Dhillon and Hoekstra, 1994; Bimbo *et al.*, 2005; Chen *et al.*, 2015), observations that are congruent with these enzymes having similar functions. However, in addition to detecting Hhp1/2 in the nucleus, in accord with their known roles in DNA damage repair, and at SPBs and the cell division site, we found that Hhp2 but not Hhp1

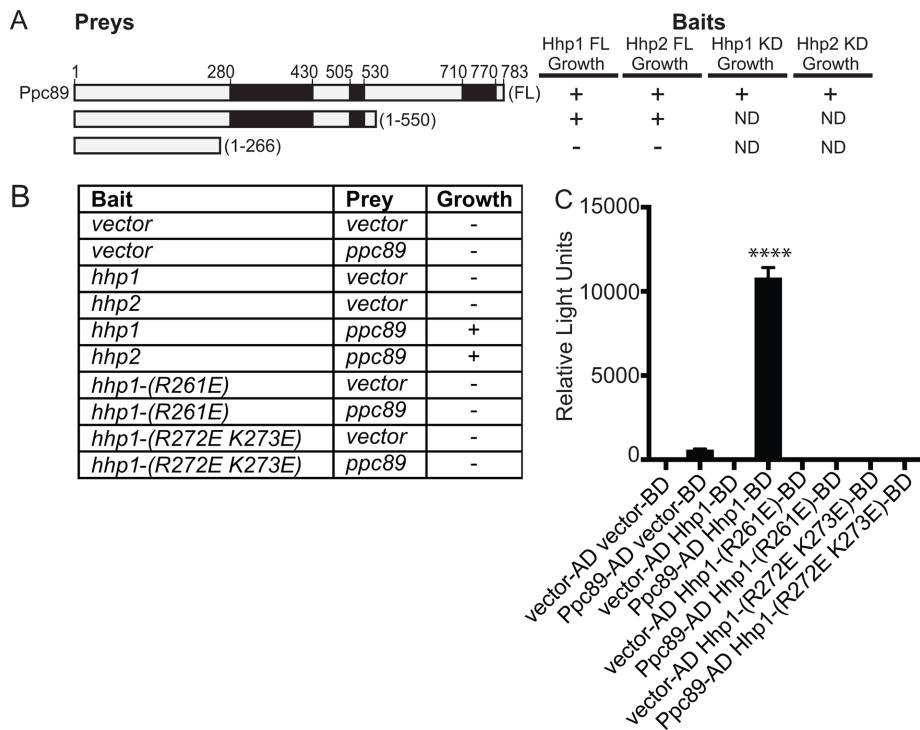


FIGURE 6: Basic residues within the kinase domain of Hhp1 are critical for interaction with the SPB protein Ppc89. (A, B) *S. cerevisiae* strain PJ69-4A was cotransformed with plasmids expressing *hhp1/2* or their variants, *hhp1*-(1-296), or *hhp2*-(1-295) and indicated sections of *ppc89*. KD = kinase domain. Black boxes in A indicate regions of predicted coiled-coil. Transformants were scored for growth on -Trp -Leu -His plates supplemented with 5 mM 3-AT. Plus signs indicate strong growth and minuses indicate no growth. (C) Bar graph shows β -galactosidase activity of the indicated bait and prey plasmids tested for growth in B (represented in relative light units). Each assay was performed in triplicate. ****, $p < 0.001$ determined using ANOVA. Error bars represent SEM.

is present at cell tips. This observation raises the possibility that these enzymes could have, in addition to common functions, variable, specialized roles that remain to be determined.

Kinase domains mediate spindle pole recruitment of Hhp1/2 and CK1 δ/ϵ

Because neither *hhp1* nor *hhp2* are essential genes (the double-deletion mutant can also be maintained; e.g., Figure 2D), we were able to clearly define the requirements for their SPB localization without the potentially confounding effects of overexpression and/or the presence of wild-type enzymes. By making gene-replacement strains producing C-terminal truncations, we pinpointed the SPB-targeting information of Hhp1/2 to within their kinase domains. In contrast, the noncatalytic C-terminus of *S. cerevisiae* Hrr25 was reported to be necessary for SPB localization (Peng *et al.*, 2015b). This difference may be explained by a “central domain” in the Hrr25 kinase that is not conserved in the *S. pombe* or mammalian CK1 enzymes and that has been found to confer functions specific to *Saccharomyces* species (Ye *et al.*, 2016). Interestingly, we found that the cell tip localization of Hhp2 is also supported by its kinase domain. Because of the high degree of sequence similarity between the Hhp1/2 kinase domains (Dhillon and Hoekstra, 1994), it seems likely that a subtle difference in the enzymes’ structures imparts this distinction in localization pattern.

Conflicting evidence has been reported regarding the requirements for CK1 δ/ϵ centrosomal targeting. While one report indicated that the kinase domain of human CK1 δ is necessary and sufficient

for proper subcellular localization (Milne *et al.*, 2001), another suggested that a C-terminal centrosomal localization sequence (equivalent to what we have termed the KDE) in mouse CK1 δ was necessary and sufficient for centrosomal localization (Greer and Rubin, 2011). Here, we found that the catalytic domains of CK1 δ/ϵ (lacking the KDEs) are sufficient for centrosome targeting, although constructs containing the KDEs are more stably localized.

In the course of characterizing the *hhp1/2* C-terminal truncation mutants, we found that removal of the C-terminal tails, but not the KDEs, led to increased catalytic activity toward an exogenous substrate in vitro. These findings agree with previous results demonstrating that phosphorylation of the C-terminal noncatalytic domain by intramolecular autophosphorylation inhibits CK1 catalytic activity (Graves and Roach, 1995; Longenecker *et al.*, 1996, 1998; Cegielska *et al.*, 1998; Gietzen and Virshup, 1999). Interestingly, *hhp1*-(1-296) and *hhp2*-(1-295) did not display any growth defects, signifying that the autoinhibition observed in vitro may not be essential in vivo, or that hypermorphic Hhp1/2 activity is not detrimental to cells. Removal of the KDEs of Hhp1/2, however, led to decreased function in vitro and in vivo. It is possible that the KDEs interact with the C-terminal lobe of the kinase domain, as does the central domain of Hrr25p (Ye *et al.*, 2016). Such an interaction could influence the structure and function of

Hhp1/2 and CK1 δ/ϵ , thereby explaining defects in both localization and activity of mutants lacking KDEs.

Hhp1/2 and CK1 δ/ϵ localize to spindle poles independently of kinase activity

We found that Hhp1/2 and CK1 δ/ϵ do not require kinase activity for SPB or centrosomal localization. This differs from what has been reported for Hrr25 (Peng *et al.*, 2015a,b) and one report on CK1 δ (Milne *et al.*, 2001). However, our results agree with another report (Qi *et al.*, 2015) indicating that CK1 δ/ϵ kinase activity is dispensable for centrosomal targeting. Because Hhp1/2 are the only protein kinases that function upstream of Dma1 in the Dma1-mediated mitotic checkpoint (Johnson *et al.*, 2013), our results indicate that Hhp1/2 do not need to phosphopriming their tether(s) at spindle poles. Thus, to accumulate at SPBs/centrosomes, these enzymes may use scaffolds whose accessibility or abundance is modulated.

Notably, only one scaffolding protein, AKAP450, has been implicated in mediating CK1 localization to centrosomes (Sillibourne *et al.*, 2002). In other signaling pathways, scaffolds are essential organizing platforms that recruit a kinase and its substrate to the same intracellular location. For example, mitogen-activated protein kinase cascades and protein kinase A pathways depend on scaffolding proteins to maintain kinase specificity (Schwartz and Madhani, 2004). In the context of Hhp1/2, which are involved in multiple cellular processes and have potentially constitutive activity, binding the scaffold Pcp89 may compartmentalize a subset of Hhp1/2 from a wider cellular population to direct CK1 enzymes to a specialized

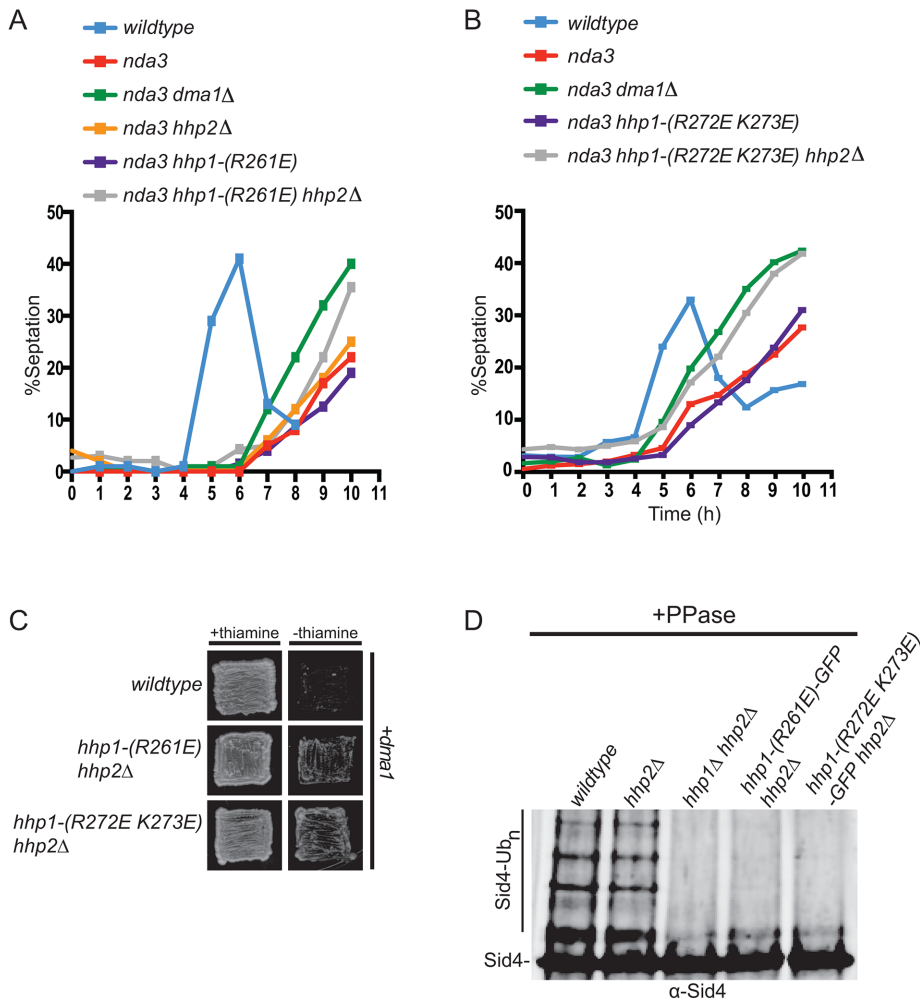


FIGURE 7: Hhp1 SPB localization is required for mitotic checkpoint function. (A, B) The indicated strains were synchronized in S phase with hydroxyurea and shifted to 19°C to activate the spindle checkpoint, and septation indices were measured periodically for 9 h. (C) Overexpression of *dma1* from the *nmt41* promoter in wild type, *hhp1-(R261E) hhp2Δ*, or *hhp1-(R272E K273E) hhp2Δ* mutant cells. Growth of the transformants was observed on agar plates in the presence (repression) or absence (derepression) of thiamine. (D) Sid4 from the indicated strains was immunoprecipitated from denatured cell lysates, treated with phosphatase, and visualized by immunoblotting.

signaling complex. Therefore, interaction with Ppc89 may 1) provide an additional level of specificity by localizing Hhp1/2 and its substrate Sid4 to the appropriate site of action, 2) generate a stronger signal by concentrating Hhp1/2 and Sid4, and/or 3) allow for coordination of the Hhp1/2-Dma1-dependent mitotic checkpoint with other signaling pathways that are centered at the SPB.

Defining the CK1 SPB-binding interface

Our results, along with previous work, indicate that CK1 catalytic domains moonlight as protein interaction domains for kinase localization. Hhp1 requires conserved basic residues on its C-terminal lobe to interact with the SPB. In only one prior case have residues in the catalytic domain of CK1 enzymes been implicated in docking interactions. Specifically, residues in the N-terminal lobe of the Hrr25p catalytic domain, together with its central domain, bind the monopolin subunit Mam1 and promote phosphorylation of monopolin's kinetochore receptor Dsn1 (Petronczki et al., 2006; Ye et al., 2016). Our findings therefore represent an important advance for the understanding of CK1 kinase domain-mediated subcellular targeting.

Though new for CK1, several other catalytic domains of broadly acting protein kinases are known to associate with scaffolds. As one example, the MAPK Fus3 is recruited and also allosterically regulated by the scaffold protein Ste5 (Choi et al., 1994; Bhattacharyya et al., 2006). Thus, Ppc89 may not only scaffold Hhp1/2 at the SPB but also modulate their catalytic activity.

Our work demonstrates that CK1 interaction with SPBs is essential for mitotic checkpoint function in *S. pombe*. Similarly, CK1δ centrosomal localization has been reported to be required for Wnt-3a-dependent neurogenesis and proper ciliogenesis (Greer and Rubin, 2011; Greer et al., 2014); thus, specific subcellular localization of CK1 enzymes is essential for mediating proper cellular signaling. Future work on the role of these enzymes at the SPB/centrosome is expected to reveal additional functions that are coordinated from this important cellular signaling nexus.

MATERIALS AND METHODS

Yeast strains, media, and genetic methods

Schizosaccharomyces pombe strains used in this study (Supplemental Table S1) were grown in yeast extract (YE) media (Moreno et al., 1991). Crosses were performed in glutamate medium (Moreno et al., 1991), and strains were constructed by tetrad analysis. *hhp1*, *hhp1-K40R*, *hhp1-R261E*, *hhp1-R272E K273E*, *hhp2*, and *cki2* were tagged endogenously at the 3' end of their open reading frames (ORFs) with *GFP:kanR* or *mNG:kanR* using pFA6 cassettes as previously described (Bahler et al., 1998). G418 (100 μg/ml; Sigma-Aldrich, St. Louis, MO) in YE media was used for selecting *kanR* cells. mNG, a recently reported GFP derived from the lancelet *Branchiostoma lanceolatum*,

was chosen for imaging experiments because of its superior brightness (Shaner et al., 2013; Willet et al., 2015). A lithium acetate transformation method (Keeney and Boeke, 1994) was used for introducing sequences encoding tags, and integration of tags was verified using whole-cell PCR and/or microscopy. Tagged *hhp1/2* alleles were fully functional as determined by growth assays and their ability to support Sid4 ubiquitination (Figure 2, D and F, and Supplemental Figures S3, C and D, and S5E). Introduction of tagged loci into other genetic backgrounds was accomplished using standard *S. pombe* mating, sporulation, and tetrad-dissection techniques. Fusion proteins were expressed from their native promoters at their normal chromosomal locus unless otherwise indicated. For *hhp1* and *hhp2* gene replacements, haploid *hhp1::ura4+* and *hhp2::ura4+* strains were transformed with linear *hhp1* and *hhp2* mutant gene fragments (digested with *Bam*HI and *Pst*I from pIRT2-*hhp1* and pIRT2-*hhp2* plasmids) using standard lithium acetate transformations. Integrants were selected based on resistance to 1.5 mg/ml 5-fluoroorotic acid (Fisher Scientific) and validated by colony PCR using primers homologous to endogenous sequences that flank the genomic clone

within pIRT2 in combination with those within the ORF. All constructs and integrants were sequenced to ensure their accuracy.

For serial-dilution growth assays, cells were cultured in liquid YE at 25°C, three serial 10-fold dilutions starting at 4×10^6 cells/ml were made, 4 μ l of each dilution was spotted on YE plates, and cells were grown at the indicated temperatures for 3–4 d. The GFP-Hhp1 (aa 280–365) fragment was cloned into a pREP81-GFP vector using *Nde*I and *Bam*HI restriction sites. This construct and a construct with GFP alone were expressed in a wild-type strain under the control of the *nmt81* promoter. Cells were grown in media containing thiamine and then washed into media without thiamine to induce protein production, then grown for 22 h at 32°C before imaging. For imaging experiments, temperature-sensitive mutants were grown at 25°C and then shifted to 36°C before imaging. Cold-sensitive *nda3-km311* strains were grown at 32°C and shifted to 19°C for 6 h, and images were acquired immediately at room temperature. All other strains were grown and imaged at 25°C.

Cell culture, transfection, fixation, and antibody staining

RPE-1 cells were cultured in DMEM/F12 supplemented with 10% fetal bovine serum and 1% penicillin/streptomycin. Cells were seeded 24 h before transfection onto 25-mm coverslips that were contained in a six-well plate. Six hours before transfection, cells were incubated in serum-free media. Plasmid DNA (1.5 μ g) was transfected into cells using Lipofectamine 3000 (Life Technologies). Cells were allowed to grow for an additional 24 h before fixation. Cells were washed once with cold 1X PBS and once with 100% cold methanol, followed by fixation with 100% cold methanol for 15 min at -20°C . Cells were then washed three times with 0.1% TBST (1X Tris-buffered saline, 0.1% Tween 20), followed by blocking with AbDil (0.1% TBST + 2% bovine serum albumin) for 10 min. Cells were stained with anti- γ -tubulin antibody (Sigma-Aldrich, GTU88; 1:500) in AbDil overnight at 4°C, washed three times with 0.1% TBST, followed by 4',6-diamidino-2-phenylindole (DAPI; 0.1 μ g/ μ l) and secondary antibody staining (Alexa Fluor 594 goat-anti mouse immunoglobulin G [IgG] [H+L], ThermoFisher; 1:500) for 45 min at 22°C. Coverslips were mounted on slides using ProLong Gold antifade mounting media (Invitrogen by ThermoFisher Scientific). Each experiment was performed in triplicate.

Molecular biology methods

All plasmids were generated by standard molecular biology techniques. *hhp1* and *hhp2* genes including 500 base pairs upstream and downstream of the ORFs were amplified by PCR and ligated into a PCR-Blunt vector (Life Technologies) and then subcloned into a pIRT2 vector (Hindley *et al.*, 1987). *hhp1* and *hhp2* mutants were created by mutagenizing pIRT2-plasmids containing *hhp1*⁺ and *hhp2*⁺ using a QuikChange site-directed mutagenesis kit (Agilent Technologies). Plasmids were validated by DNA sequencing.

The ORF of CK1 δ was amplified by PCR from a plasmid (CK1 δ pGEX-6p-2) kindly provided by Fanni Gergely (University of Cambridge). V405 4HA-CK1 ϵ , a gift from David Virshup (Duke University Medical School) (Addgene plasmid #13724), was used as a template for PCR amplification of the CK1 ϵ ORF. Each PCR product was cloned into pEGFP-C1, and the correct sequence was validated by DNA sequencing. Mutant CK1 δ/ϵ variants were made using the QuikChange site-directed mutagenesis kit (Agilent Technologies) and confirmed by DNA sequencing.

Schizosaccharomyces pombe protein methods

Cell pellets were frozen in a dry ice/ethanol bath and lysed by bead disruption in NP-40 lysis buffer under denaturing SDS lysis

conditions as previously described (Gould *et al.*, 1991), except with the addition of a complete protease inhibitor mixture (Calbiochem). Cell pellets for Hhp1 and Hhp2 immunoblots were lysed by bead disruption using a FastPrep cell homogenizer (MP Biomedicals). For analysis of Sid4 ubiquitination, Sid4 was immunoprecipitated under denaturing SDS conditions using Sid4 antiserum (Johnson *et al.*, 2013). Proteins were separated on a 4–12% Bis-Tris gel (Life Technologies), transferred to Immobilon-P polyvinylidene fluoride (Millipore) membrane, and immunoblotted with anti-GFP (Roche, 1:1000), anti-Sid4 (1:2000), and fluorescent anti-mouse and anti-rabbit secondary antibodies (Li-Cor Biosciences) according to the manufacturers' instructions.

Microscopy methods

Live-cell images of *S. pombe* cells were acquired using a Personal DeltaVision microscope system (Applied Precision) that includes an Olympus IX71 microscope, 60 \times /1.42 NA Plan-Apo and 100 \times /1.40 NA UPlanSApo objectives, a Photometrics CoolSnap HQ2 camera, and softWoRx imaging software. Images in figures are maximum-intensity projections of z-sections spaced at 0.2–0.5 μ m. Images used for quantification were not deconvolved and were sum projected. Other images were deconvolved with 10 iterations. Time-lapse imaging was performed on cells in log phase using a microfluidics perfusion system (CellASIC ONIX; EMD Millipore). Cells were loaded into Y04C plates for 5 s at 8 psi, and YE liquid medium was flowed into the chamber at 5 psi throughout imaging. Quantitative analysis of microscopy data was performed using Fiji (a version of ImageJ software available at <https://fiji.sc>). For comparison of populations of cells for all genotypes, cells were imaged on the same day with the same microscope parameters. The average mNG fluorescence intensity of each protein at SPBs was measured in at least 20 cells. For all intensity measurements, the background was subtracted by creating a region of interest (ROI) in the same image where there were no cells. The raw intensity of the background was divided by the area of the background, which was multiplied by the area of the ROI. This number was subtracted from the raw integrated intensity of that ROI. For SPB intensity quantification, an ROI was drawn around the SPB and measured for raw integrated density; for whole-cell intensity quantification, an ROI was drawn around the entire cell. The average mCherry fluorescence intensities were measured similarly, and final values for each cell are expressed as mNG/mCherry ratios. Measurements for the 20 cells in each group were averaged for statistical analysis using a two-tailed Student's *t* test or analysis of variance (ANOVA) implemented in Prism 6 (GraphPad Software). All statistical ANOVAs used Tukey's post hoc analysis.

In addition, for comparison of two populations of cells within the same field of view, one population was incubated with fluorescently conjugated lectin (Sigma-Aldrich), which labels cell walls. Specifically, 1 μ l of a 5 mg/ml stock of tetramethylrhodamine-lectin in water was added to 1 ml of cells for a final concentration of 5 μ g/ml. Cells were then incubated for 10 min at room temperature, washed three times, and resuspended in media. The lectin-labeled cell population and unlabeled cell population were mixed 1:1 immediately before imaging. The reciprocal labeling of populations was also performed to account for any signal bleed-through. The fluorescence intensity of the SPB was quantified, and background fluorescence was subtracted (Willet *et al.*, 2015).

In vitro kinase assays

MBP-Hhp1 and MBP-Hhp2 fusion proteins were purified on amylose beads (New England Biolabs) in column buffer (20 mM Tris, pH

7.0, 150 mM NaCl, 2 mM EDTA, and 0.1% NP40) and eluted with maltose (10 mM). Kinase reactions were performed with 500 ng kinase, 500 ng casein, 10 μ M ATP plus 1 μ Ci γ -[32 P]ATP in kinase buffer (50 mM Tris, pH 7.5, 10 mM MgCl₂, and 5 mM dithiothreitol) in 20 μ l at 30°C for 30 min. Reactions were quenched by adding SDS-PAGE sample buffer, and proteins were separated by SDS-PAGE. Phosphorylated proteins were visualized by autoradiography, and relative protein quantities were assessed by Coomassie blue staining relative to known standards using Odyssey software (Li-Cor Biosciences). Kinetic assays were performed using recombinant MBP-Hhp1 and MBP-Hhp2 fusion proteins treated for 2 h with lambda phosphatase (New England Biolabs). These kinase reactions were performed with 0.25 μ M of kinase, 25 μ M casein, 5 μ M cold ATP, 2 μ Ci [32 P]-ATP in CK1 kinase buffer. Reactions were quenched at different time points by adding SDS sample buffer, and proteins were separated by SDS-PAGE. Phosphorylated proteins were visualized and quantitated using an FLA7000IP Typhoon Storage Phosphorimager (GE Healthcare Life Sciences). Kinetic measurements were calculated using Prism 6 software. Relative protein quantities were assessed by Coomassie blue staining.

Two-hybrid analyses

Two-hybrid experiments were performed as described previously (Vo *et al.*, 2016). *hhp1* and *ppc89*, cloned into pDEST DB and pDEST AD vectors, respectively, were generously provided by Haiyuan Yu (Cornell University). These or fragments thereof were cotransformed into *S. cerevisiae* strain PJ69-4A. Leu⁺ and Trp⁺ transformants were selected and then scored for positive interactions by streaking onto synthetic dextrose plates containing 5 mM 3-amino-1,2,4-triazole and lacking tryptophan, leucine, and histidine. β -Galactosidase reporter enzyme activity in the two-hybrid strains was measured using the Galacto-Star chemiluminescent reporter assay system according to the manufacturer's instructions (Applied Biosystems, Foster City, CA), except that cells were lysed by glass bead disruption. Each experiment was performed in triplicate. Reporter assays were recorded on a Multi-Detection Microplate Reader (Bio-TEK Instruments).

Checkpoint assay

Schizosaccharomyces pombe cells were synchronized in S phase using hydroxyurea (HU; Sigma) at a final concentration of 12 mM for 3–3.5 h at 32°C. Cells were then filtered into HU-free media and immediately incubated at 19°C to activate the spindle checkpoint. Cells were fixed in 70% ethanol, and septation indices were measured periodically for 10 h by methyl blue staining of the septa.

Protein modeling

Structural models of Hhp1 and Cki2 were generated using the Protein Homology/analogy Recognition Engine v. 2.0 (Phyre²) (Kelley *et al.*, 2015). Homology models were generated from crystal structures of the kinase domains of Hhp1 and Cki2 homologues.

ACKNOWLEDGMENTS

We thank Sierra Cullati, Jun-Song Chen, Alaina Willet, Christine Jones, and Janel Beckley for critical comments on the article. Liping Ren and Jun-Song Chen are thanked for outstanding technical assistance. pDEST two-hybrid vectors were a gracious gift from the Yu lab (Weill Institute for Cell and Molecular Biology, Cornell University). Z.C.E. was supported by the Integrated Biological Systems Training in Oncology Program (2T32CA119925-06). R.X.G. was supported by the Vanderbilt Initiative for Maximizing Student Diversity

program (R25 5R25GM062459-11). This work was funded by National Institutes of Health grant R01GM112989 to K.L.G.

REFERENCES

- Agostinis P, Pinna LA, Meggio F, Marin O, Goris J, Vandenheede JR, Merlevede W (1989). A synthetic peptide substrate specific for casein kinase I. *FEBS Lett* 259, 75–78.
- Babu P, Bryan JD, Panek HR, Jordan SL, Forbrich BM, Kelley SC, Colvin RT, Robinson LC (2002). Plasma membrane localization of the Yck2p yeast casein kinase 1 isoform requires the C-terminal extension and secretory pathway function. *J Cell Sci* 115, 4957–4968.
- Babu P, Deschenes RJ, Robinson LC (2004). Akr1p-dependent palmitoylation of Yck2p yeast casein kinase 1 is necessary and sufficient for plasma membrane targeting. *J Biol Chem* 279, 27138–27147.
- Bahler J, Wu JQ, Longtine MS, Shah NG, McKenzie A 3rd, Steever AB, Wach A, Philippsen P, Pringle JR (1998). Heterologous modules for efficient and versatile PCR-based gene targeting in *Schizosaccharomyces pombe*. *Yeast* 14, 943–951.
- Bhattacharyya RP, Remenyi A, Good MC, Bashor CJ, Falick AM, Lim WA (2006). The Ste5 scaffold allosterically modulates signaling output of the yeast mating pathway. *Science* 311, 822–826.
- Bimbo A, Jia Y, Poh SL, Karuturi RK, den Elzen N, Peng X, Zheng L, O'Connell M, Liu ET, Balasubramanian MK, Liu J (2005). Systematic deletion analysis of fission yeast protein kinases. *Eukaryot Cell* 4, 799–813.
- Carmel G, Leichus B, Cheng X, Patterson SD, Mirza U, Chait BT, Kuret J (1994). Expression, purification, crystallization, and preliminary x-ray analysis of casein kinase-1 from *Schizosaccharomyces pombe*. *J Biol Chem* 269, 7304–7309.
- Carpay A, Krug K, Graf S, Koch A, Popic S, Hauf S, Macek B (2014). Absolute proteome and phosphoproteome dynamics during the cell cycle of *Schizosaccharomyces pombe* (fission yeast). *Mol Cell Proteomics* 13, 1925–1936.
- Cegielska A, Gietzen KF, Rivers A, Virshup DM (1998). Autoinhibition of casein kinase I epsilon (CKI epsilon) is relieved by protein phosphatases and limited proteolysis. *J Biol Chem* 273, 1357–1364.
- Chan KY, Alonso-Nunez M, Grallert A, Tanaka K, Connolly Y, Smith DL, Hagan IM (2017). Dialogue between centrosomal entrance and exit scaffold pathways regulates mitotic commitment. *J Cell Biol* 216, 2795–2812.
- Chang L, Gould KL (2000). Sid4p is required to localize components of the septation initiation pathway to the spindle pole body in fission yeast. *Proc Natl Acad Sci USA* 97, 5249–5254.
- Chen JS, Beckley JR, McDonald NA, Ren L, Mangione M, Jang SJ, Elmore ZC, Rachfall N, Feoktistova A, Jones CM, *et al.* (2015). Identification of new players in cell division, DNA damage response, and morphogenesis through construction of *Schizosaccharomyces pombe* deletion strains. *G3 (Bethesda)* 5, 361–370.
- Choi KY, Satterberg B, Lyons DM, Elion EA (1994). Ste5 tethers multiple protein kinases in the MAP kinase cascade required for mating in *S. cerevisiae*. *Cell* 78, 499–512.
- Dahlberg CL, Nguyen EZ, Goodlett D, Kimelman D (2009). Interactions between Casein kinase Ie (CKIe) and two substrates from disparate signaling pathways reveal mechanisms for substrate-kinase specificity. *PLoS One* 4, e4766.
- Desjardins PR, Lue PF, Liew CC, Gornall AG (1972). Purification and properties of rat liver nuclear protein kinases. *Can J Biochem* 50, 1249–1259.
- Dhillon N, Hoekstra MF (1994). Characterization of two protein kinases from *Schizosaccharomyces pombe* involved in the regulation of DNA repair. *EMBO J* 13, 2777–2788.
- Flotow H, Graves PR, Wang AQ, Fiol CJ, Roeske RW, Roach PJ (1990). Phosphate groups as substrate determinants for casein kinase I action. *J Biol Chem* 265, 14264–14269.
- Flotow H, Roach PJ (1991). Role of acidic residues as substrate determinants for casein kinase I. *J Biol Chem* 266, 3724–3727.
- Ghalei H, Schaub FX, Doherty JR, Noguchi Y, Roush WR, Cleveland JL, Stroupe ME, Karbstein K (2015). Hrr25/CK1 δ -directed release of Lt1 from pre-40S ribosomes is necessary for ribosome assembly and cell growth. *J Cell Biol* 208, 745–759.
- Gietzen KF, Virshup DM (1999). Identification of inhibitory autophosphorylation sites in casein kinase I epsilon. *J Biol Chem* 274, 32063–32070.
- Gould KL, Moreno S, Owen DJ, Sazer S, Nurse P (1991). Phosphorylation at Thr167 is required for *Schizosaccharomyces pombe* p34cdc2 function. *EMBO J* 10, 3297–3309.
- Graves PR, Haas DW, Hagedorn CH, DePaoli-Roach AA, Roach PJ (1993). Molecular cloning, expression, and characterization of a 49-kilodalton casein kinase I isoform from rat testis. *J Biol Chem* 268, 6394–6401.

- Graves PR, Roach PJ (1995). Role of COOH-terminal phosphorylation in the regulation of casein kinase I delta. *J Biol Chem* 270, 21689–21694.
- Greer YE, Rubin JS (2011). Casein kinase I delta functions at the centrosome to mediate Wnt-3a-dependent neurite outgrowth. *J Cell Biol* 192, 993–1004.
- Greer YE, Westlake CJ, Gao B, Bharti K, Shiba Y, Xavier CP, Pazour GJ, Yang Y, Rubin JS (2014). Casein kinase 1δ functions at the centrosome and Golgi to promote ciliogenesis. *Mol Biol Cell* 25, 1629–1640.
- Guertin DA, Venkatram S, Gould KL, McCollum D (2002). Dma1 prevents mitotic exit and cytokinesis by inhibiting the septation initiation network (SIN). *Dev Cell* 3, 779–790.
- Hathaway GM, Traugh JA (1979). Cyclic nucleotide-independent protein kinases from rabbit reticulocytes. Purification of casein kinases. *J Biol Chem* 254, 762–768.
- Hindley J, Phear G, Stein M, Beach D (1987). *Suc1⁺* encodes a predicted 13-kilodalton protein that is essential for cell viability and is directly involved in the division cycle of *Schizosaccharomyces pombe*. *Mol Cell Biol* 7, 504–511.
- Hoekstra MF, Dhillon N, Carmel G, DeMaggio AJ, Lindberg RA, Hunter T, Kuret J (1994). Budding and fission yeast casein kinase I isoforms have dual-specificity protein kinase activity. *Mol Biol Cell* 5, 877–886.
- Hutchins JR, Toyoda Y, Hegemann B, Poser I, Heriche JK, Sykora MM, Augsburg M, Hudecz O, Buschhorn BA, Bulkescher J, et al. (2010). Systematic analysis of human protein complexes identifies chromosome segregation proteins. *Science* 328, 593–599.
- lanes C, Xu P, Werz N, Meng Z, Henne-Bruns D, Bischof J, Knippschild U (2015). CK1δ activity is modulated by CDK2/E- and CDK5/p35-mediated phosphorylation. *Amino Acids* 48, 579–592.
- Johnson AE, Chen JS, Gould KL (2013). CK1 is required for a mitotic checkpoint that delays cytokinesis. *Curr Biol* 23, 1920–1926.
- Johnson AE, Gould KL (2011). Dma1 ubiquitinates the SIN scaffold, Sid4, to impede the mitotic localization of Plo1 kinase. *EMBO J* 30, 341–354.
- Johnson AE, McCollum D, Gould KL (2012). Polar opposites: fine-tuning cytokinesis through SIN asymmetry. *Cytoskeleton (Hoboken)* 69, 686–699.
- Keeney JB, Boeke JD (1994). Efficient targeted integration at *leu1-32* and *ura4-294* in *Schizosaccharomyces pombe*. *Genetics* 136, 849–856.
- Kelley LA, Mezulis S, Yates CM, Wass MN, Sternberg MJ (2015). The Phyre2 web portal for protein modeling, prediction and analysis. *Nat Protoc* 10, 845–858.
- Knippschild U, Gocht A, Wolff S, Huber N, Lohler J, Stoter M (2005). The casein kinase 1 family: participation in multiple cellular processes in eukaryotes. *Cell Signal* 17, 675–689.
- Knippschild U, Kruger M, Richter J, Xu P, Garcia-Reyes B, Peifer C, Halekotte J, Bakulev V, Bischof J (2014). The CK1 family: contribution to cellular stress response and its role in carcinogenesis. *Front Oncol* 4, 96.
- Longenecker KL, Roach PJ, Hurley TD (1996). Three-dimensional structure of mammalian casein kinase I: molecular basis for phosphate recognition. *J Mol Biol* 257, 618–631.
- Longenecker KL, Roach PJ, Hurley TD (1998). Crystallographic studies of casein kinase I delta toward a structural understanding of auto-inhibition. *Acta Crystallogr D Biol Crystallogr* 54, 473–475.
- Marguerat S, Schmidt A, Codlin S, Chen W, Aebbersold R, Bahler J (2012). Quantitative analysis of fission yeast transcriptomes and proteomes in proliferating and quiescent cells. *Cell* 151, 671–683.
- Matsumura S, Takeda M (1972). Phosphoprotein kinases from rat liver cytosol. *Biochim Biophys Acta* 289, 237–241.
- Matsuyama A, Arai R, Yashiroda Y, Shirai A, Kamata A, Sekido S, Kobayashi Y, Hashimoto A, Hamamoto M, Hiraoka Y, et al. (2006). ORFome cloning and global analysis of protein localization in the fission yeast *Schizosaccharomyces pombe*. *Nat Biotechnol* 24, 841–847.
- Meggio F, Perich JW, Marin O, Pinna LA (1992). The comparative efficiencies of the Ser(P)-, Thr(P)- and Tyr(P)-residues as specificity determinants for casein kinase-1. *Biochem Biophys Res Commun* 182, 1460–1465.
- Meggio F, Perich JW, Reynolds EC, Pinna LA (1991). A synthetic beta-casein phosphopeptide and analogues as model substrates for casein kinase-1, a ubiquitous, phosphate directed protein kinase. *FEBS Lett* 283, 303–306.
- Meng Z, Bischof J, lanes C, Henne-Bruns D, Xu P, Knippschild U (2016). CK1δ kinase activity is modulated by protein kinase C alpha (PKCα)-mediated site-specific phosphorylation. *Amino Acids* 48, 1185–1197.
- Milne DM, Looby P, Meek DW (2001). Catalytic activity of protein kinase CK1δ (casein kinase 1δ) is essential for its normal subcellular localization. *Exp Cell Res* 263, 43–54.
- Moreno S, Klar A, Nurse P (1991). Molecular genetic analysis of fission yeast *Schizosaccharomyces pombe*. *Methods Enzymol* 194, 795–823.
- Murone M, Simanis V (1996). The fission yeast *dma1* gene is a component of the spindle assembly checkpoint, required to prevent septum formation and premature exit from mitosis if spindle function is compromised. *EMBO J* 15, 6605–6616.
- Nakatogawa H (2015). Hrr25: an emerging major player in selective autophagy regulation in *Saccharomyces cerevisiae*. *Autophagy* 11, 432–433.
- Peng Y, Grassart A, Lu R, Wong CC, Yates J 3rd, Barnes G, Drubin DG (2015a). Casein kinase 1 promotes initiation of clathrin-mediated endocytosis. *Dev Cell* 32, 231–240.
- Peng Y, Moritz M, Han X, Giddings TH, Lyon A, Kollman J, Winey M, Yates J 3rd, Agard DA, Drubin DG, Barnes G (2015b). Interaction of CK1δ with γTuSC ensures proper microtubule assembly and spindle positioning. *Mol Biol Cell* 26, 2505–2518.
- Petronczki M, Matos J, Mori S, Gregan J, Bogdanova A, Schwickart M, Mechtler K, Shirahige K, Zachariae W, Nasmyth K (2006). Monopolar attachment of sister kinetochores at meiosis I requires casein kinase 1. *Cell* 126, 1049–1064.
- Qi ST, Wang ZB, Huang L, Liang LF, Xian YX, Ouyang YC, Hou Y, Sun QY, Wang WH (2015). Casein kinase 1 (α, δ and ε) localize at the spindle poles, but may not be essential for mammalian oocyte meiotic progression. *Cell Cycle* 14, 1675–1685.
- Rosenberg JA, Tomlin GC, McDonald WH, Snydsman BE, Muller EG, Yates JR 3rd, Gould KL (2006). Ppc89 links multiple proteins, including the septation initiation network, to the core of the fission yeast spindle-pole body. *Mol Biol Cell* 17, 3793–3805.
- Sakuno T, Watanabe Y (2015). Phosphorylation of cohesin Rec11/SA3 by casein kinase 1 promotes homologous recombination by assembling the meiotic chromosome axis. *Dev Cell* 32, 220–230.
- Schitteck B, Sinnberg T (2014). Biological functions of casein kinase 1 isoforms and putative roles in tumorigenesis. *Mol Cancer* 13, 231.
- Schwartz MA, Madhani HD (2004). Principles of MAP kinase signaling specificity in *Saccharomyces cerevisiae*. *Annu Rev Genet* 38, 725–748.
- Shaner NC, Lambert GG, Chammas A, Ni Y, Cranfill PJ, Baird MA, Sell BR, Allen JR, Day RN, Israelsson M, et al. (2013). A bright monomeric green fluorescent protein derived from *Branchiostoma lanceolatum*. *Nat Methods* 10, 407–409.
- Sillibourne JE, Milne DM, Takahashi M, Ono Y, Meek DW (2002). Centrosomal anchoring of the protein kinase CK1δ mediated by attachment to the large, coiled-coil scaffolding protein CG-NAP/AKAP450. *J Mol Biol* 322, 785–797.
- Simanis V (2015). Pombe's thirteen—control of fission yeast cell division by the septation initiation network. *J Cell Sci* 128, 1465–1474.
- Sun B, Chen L, Cao W, Roth AF, Davis NG (2004). The yeast casein kinase Yck3p is palmitoylated, then sorted to the vacuolar membrane with AP-3-dependent recognition of a YXXΦ adaptin sorting signal. *Mol Biol Cell* 15, 1397–1406.
- Toda T, Umesono K, Hirata A, Yanagida M (1983). Cold-sensitive nuclear division arrest mutants of the fission yeast *Schizosaccharomyces pombe*. *J Mol Biol* 168, 251–270.
- Tuazon PT, Traugh JA (1991). Casein kinase I and II—multipotential serine protein kinases: structure, function, and regulation. *Adv Second Messenger Phosphoprotein Res* 23, 123–164.
- Vancura A, Sessler A, Leichus B, Kuret J (1994). A prenylation motif is required for plasma membrane localization and biochemical function of casein kinase I in budding yeast. *J Biol Chem* 269, 19271–19278.
- Vo TV, Das J, Meyer MJ, Cordero NA, Akturk N, Wei X, Fair BJ, Degatano AG, Fragoza R, Liu LG, et al. (2016). A proteome-wide fission yeast interactome reveals network evolution principles from yeasts to human. *Cell* 164, 310–323.
- Wang PC, Vancura A, Mitcheson TG, Kuret J (1992). Two genes in *Saccharomyces cerevisiae* encode a membrane-bound form of casein kinase-1. *Mol Biol Cell* 3, 275–286.
- Willet AH, McDonald NA, Bohnert KA, Baird MA, Allen JR, Davidson MW, Gould KL (2015). The F-BAR Cdc15 promotes contractile ring formation through the direct recruitment of the formin Cdc12. *J Cell Biol* 208, 391–399.
- Xu RM, Carmel G, Sweet RM, Kuret J, Cheng X (1995). Crystal structure of casein kinase-1, a phosphate-directed protein kinase. *EMBO J* 14, 1015–1023.
- Ye Q, Ur SN, Su TY, Corbett KD (2016). Structure of the *Saccharomyces cerevisiae* Hrr25:Mam1 monopolin subcomplex reveals a novel kinase regulator. *EMBO J* 35, 2139–2151.